

Optical-Model Analysis of High-Energy Neutrons Scattered by Deformed Nuclei

E. GARY CORMAN

Lawrence Radiation Laboratory, University of California, Livermore, California

(Received August 28, 1961)

This work investigates the effects of target nuclear deformations upon the high-energy differential elastic and rotational excitation cross sections for neutron scattering. An optical-model potential of cylindrically symmetrical ellipsoidal shape is used to represent the target nucleus. The deformed potential is first oriented parallel to each of the coordinate axes. The differential cross sections are evaluated and averaged over such orientations. Next, the potential is oriented at an arbitrary angle. The differential cross section is evaluated and averaged over all possible orientation angles. The foregoing averaged cross sections are compared with the cross sections obtained by assuming spherical nuclei for the cases of aluminum and lutetium. Third, differential cross sections with the simultaneous excitations of the target nucleus to higher rotational levels are investigated. Results of calculations are shown for a nucleus having the dimensions of lutetium in initial $I=0$ and $I=7$ spin states. Fourth, the cross section and polarization are investigated by assuming a spin-orbit interaction added to the central deformed potential. It is found that for an arbitrary nuclear orientation the polarization generally has a component parallel to the scattering plane. However, such a component vanishes upon averaging over orientations.

I. INTRODUCTION

IT is useful to consider those aspects of high-energy nuclear scattering which can be represented by formulations independent of the detailed individual nucleon collisions that occur during a nucleon-nuclear scattering. It seems reasonable to expect that in the high-energy neutron range ($\gtrsim 100$ Mev), the elastic cross sections can be adequately described in terms of "macroscopic" parameters, which can be considered to represent averages over the detailed "microscopic" processes.

It has long been known that nuclei in certain mass ranges possess deformations from sphericity. The primary purpose of this work is to investigate the effects of the target nuclear deformations upon the high-energy differential elastic and rotational cross sections for neutron-nuclear scattering. In applying the macroscopic model to scattering processes on deformed nuclei, the detailed nuclear structure is replaced by an equivalent ellipsoid-shaped complex potential region, (i.e., the optical model representation). The imaginary part of the potential describes the totality of all microscopic inelastic scattering and absorption.

At high energies, experiments indicate that the only appreciable scattering occurs in the small solid angle about the forward direction. The following integral expression derived by Schiff¹ and Glauber,² and valid for small-angle scattering, was therefore used:

$$f(\mathbf{k}_0, \mathbf{k}_f) = \frac{ik}{2\pi} \int_{-\infty}^{+\infty} \int_{-\infty}^{+\infty} e^{i(q_x x + q_y y)} \times \left\{ 1 - \exp \left[(-ik/2E) \int_{-\infty}^{+\infty} V(x, y, z) dz \right] \right\} dx dy, \quad (1)$$

where k and E are the initial momentum wave number

and energy of the neutron, $V(\mathbf{r})$ the nuclear potential felt by the neutron, and $\mathbf{q} = \mathbf{k}_0 - \mathbf{k}_f$, in which \mathbf{k}_0 and \mathbf{k}_f are the incoming and outgoing momentum wave vectors. For the calculated results shown in the following sections, a cylindrically symmetrical deformed potential of semimajor axis b and semiminor axis c was used. It has the following analytical form (if the nucleus were spherical of radius R):

$$V(r) = -(V_0 + iW_0)(1 - r^2/R^2)^{\frac{1}{2}}, \quad r \leq R, \\ V(r) = 0, \quad r > R.$$

The potential depths V_0 and W_0 were chosen from other works³ that employed optical-model calculations, and in such a way that the total cross section equals that which resulted from using a square-well potential. Parameters b and c were found by holding the nuclear volume constant as the nucleus is deformed from sphericity.

II. ELASTIC CROSS-SECTION CLASSICAL AVERAGE OVER DISCRETE ORIENTATIONS

Letting the scattering plane lie in the x - z plane and $\mathbf{k}_0 + \mathbf{k}_f$ in the z direction as shown in Fig. 1, integral (1) was evaluated for the three cases of the symmetry axis of the ellipsoid oriented along the x , y , and z axes. A classical cross-sectional average over these three discrete orientations should compare favorably with the cross section obtained by integrating over all possible orientation angles (see Sec. III).

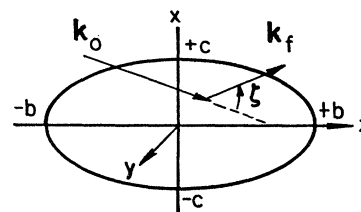


FIG. 1. Nucleus oriented along z axis.

¹ L. I. Schiff, Phys. Rev. **103**, 443 (1956).

² R. J. Glauber, *Lectures in Theoretical Physics* (Interscience Publishers, Inc., New York, 1959), Vol. 1, p. 315.

³ I. Shapiro, dissertation, Harvard University, Cambridge, Massachusetts, 1955 (unpublished).

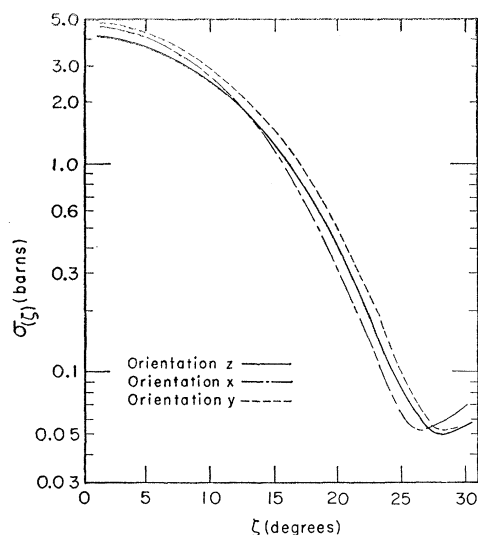


FIG. 2. Differential elastic cross section vs angle for 84-Mev neutrons scattered by aluminum; $b=4.94$ f, $c=4.59$ f, $V_0+iW_0=38.2+i14.0$ Mev.

For the ellipsoid oriented along the z axis, one may change directly to cylindrical coordinates and obtain for (1):

$$f_z = \frac{c}{2i \sin(\zeta/2)} \sum_{n=1}^{\infty} \left[\frac{2i\Delta}{2kc \sin(\zeta/2)} \right]^n \times J_{n+1}[2kc \sin(\zeta/2)], \quad (2)$$

where $\Delta = (\pi/4)kb(V_0+iW_0)/E$, and $J_n(x)$ is a Bessel function of order n , and ζ is the angle between \mathbf{k}_0 and \mathbf{k}_f .

For orientations x and y , one may change coordinates in such a way that cylindrical symmetry exists about the z axis. One obtains

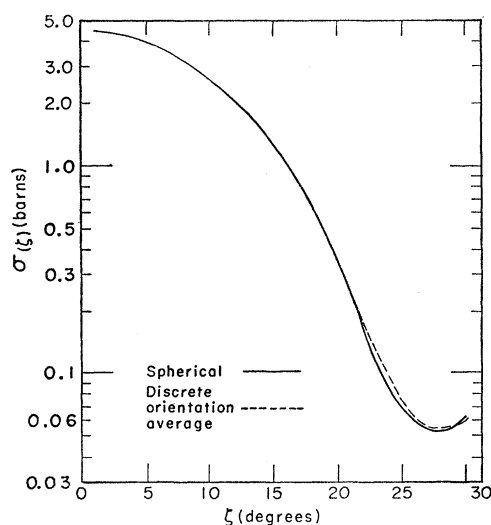


FIG. 3. Differential elastic cross section vs angle for 84-Mev neutrons scattered by aluminum; $b=4.94$ f, $c=4.59$ f, $V_0+iW_0=38.2+i14.0$ Mev.

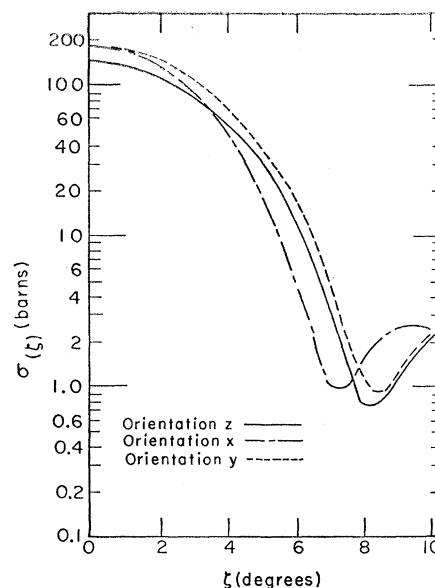


FIG. 4. Differential elastic cross section vs angle for 200-Mev neutrons scattered by lutetium; $b=10.67$ f, $c=9.17$ f, $V_0+iW_0=24.1+i18.7$ Mev.

$$f_x = \frac{c}{2i \sin(\zeta/2)} \sum_{n=1}^{\infty} \left[\frac{2i\delta}{2kb \sin(\zeta/2)} \right]^n \times J_{n+1}[2kb \sin(\zeta/2)], \quad (3)$$

and

$$f_y = \frac{b}{2i \sin(\zeta/2)} \sum_{n=1}^{\infty} \left[\frac{2i\delta}{2kc \sin(\zeta/2)} \right]^n \times J_{n+1}[2kc \sin(\zeta/2)], \quad (4)$$

where $\delta = (\pi/4)kc(V_0+iW_0)/E$.

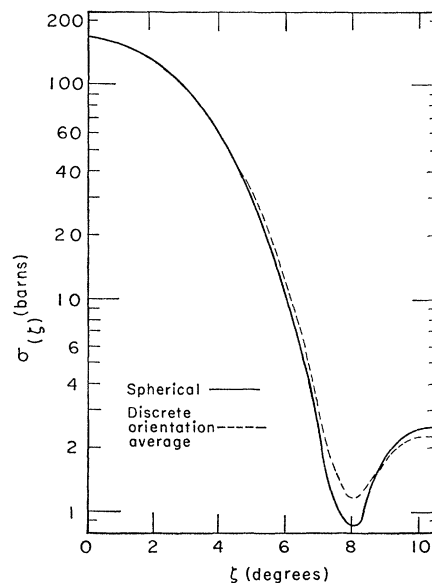


FIG. 5. Differential elastic cross section vs angle for 200-Mev neutrons scattered by lutetium; $b=10.67$ f, $c=9.17$ f, $V_0+iW_0=24.1+i18.7$ Mev.

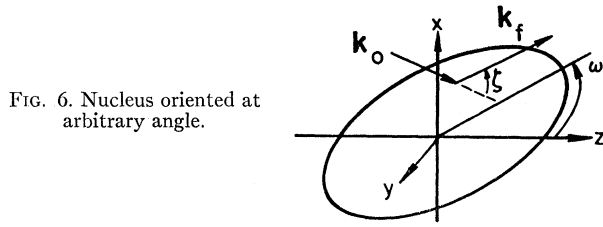


FIG. 6. Nucleus oriented at arbitrary angle.

Figures 2 and 4 show the results of the differential elastic cross-section calculations for the three orientations, which were obtained using formulas (2), (3), and (4) by multiplying the scattering amplitude by its complex conjugate. Figures 3 and 5 compare the cross-sectional average over orientations with the cross section for the corresponding spherical nucleus.

III. ELASTIC CROSS SECTION CONTINUOUSLY AVERAGED OVER ORIENTATION

The scattering-amplitude integral of Schiff will now be solved for a nucleus oriented at an arbitrary angle, as shown in Fig. 6. Let the ellipsoid be oriented at an arbitrary angle ω , which is composed of the polar angle θ and the azimuthal angle ϕ . It is assumed that the nucleus does not precess appreciably during the scattering ("adiabatic approximation").⁴ This approximation is well justified because of the high neutron energies considered.

The integration variables in (1) were transformed in such a way that the ellipsoid became a sphere. After effecting the necessary transformations, defining the deformation parameter $\epsilon \equiv (b/c) - 1$, ignoring all powers

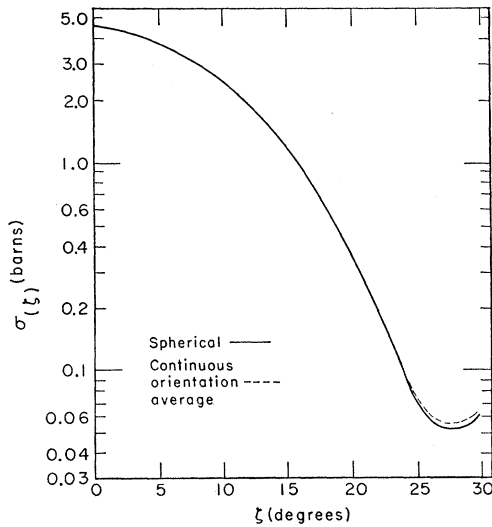


FIG. 7. Elastic scattering of 84-Mev neutrons by aluminum.

⁴ W. Pauli, *Die Allgemeinen Prinzipien der Wellenmechanik* (Edwards Brothers, Inc., Ann Arbor, Michigan, 1947), p. 161.

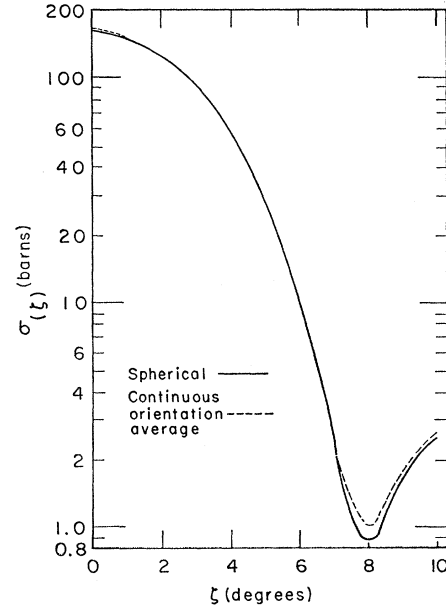


FIG. 8. Elastic scattering of 200-Mev neutrons by lutetium.

of ϵ greater than two, and integrating:

$$f(\xi, \theta, \phi) = (kc^2/i) \{ A + \epsilon(A \sin^2 \theta - B \sin^2 \theta \cos^2 \phi + C \cos^2 \theta) + \epsilon^2 [-D \cos^4 \theta + C \sin^2 \theta \cos^2 \theta - B [(\sin^4 \theta \cos^2 \phi \sin^2 \phi) / 2 + \sin^4 \theta \cos^2 \phi] - E \cos^2 \theta \sin^2 \theta \cos^2 \phi + F \sin^4 \theta \cos^4 \phi - G \sin^4 \theta \cos^4 \phi] \}, \quad (5)$$

where A through G have the following definitions:

$$A \equiv \int_0^{\pi/2} J_0(\alpha \sin \tau) [\exp(i\beta \cos^2 \tau) - 1] \sin \tau \cos \tau d\tau,$$

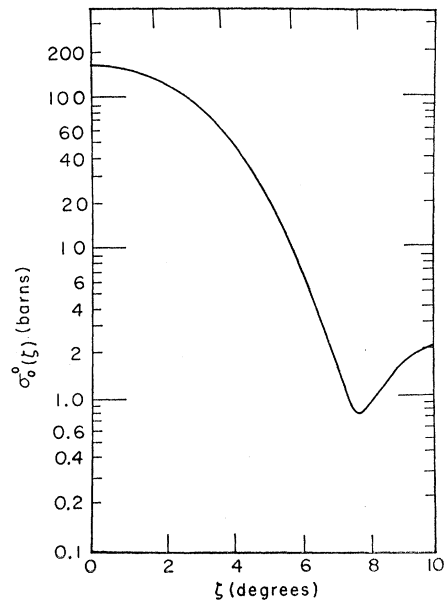


FIG. 9. Rotational scattering of 200-Mev neutrons by lutetium.

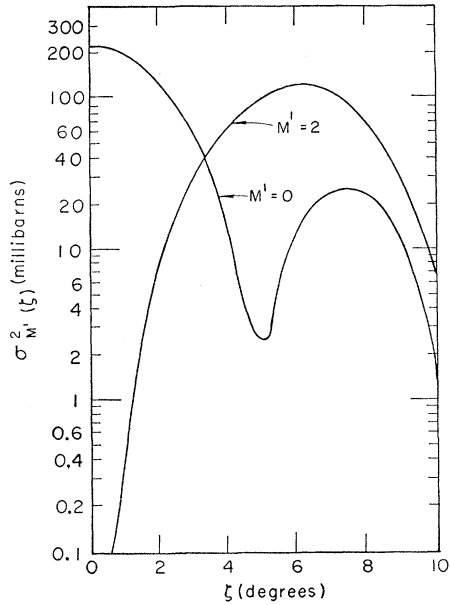


FIG. 10. Rotational scattering of 200-Mev neutrons by lutetium.

$$B \equiv \alpha \int_0^{\pi/2} J_1(\alpha \sin \tau) [\exp(i\beta \cos^2 \tau) - 1] \sin^2 \tau \cos \tau d\tau,$$

$$C \equiv i\beta \int_0^{\pi/2} J_0(\alpha \sin \tau) \exp(i\beta \cos^2 \tau) \cos^3 \tau \sin \tau d\tau,$$

$$D \equiv \beta^2/2 \int_0^{\pi/2} J_0(\alpha \sin \tau) \exp(i\beta \cos^2 \tau) \cos^5 \tau \sin \tau d\tau,$$

$$E \equiv \alpha i\beta \int_0^{\pi/2} J_1(\alpha \sin \tau) \exp(i\beta \cos^2 \tau) \cos^3 \tau \sin^2 \tau d\tau,$$

$$F \equiv \alpha^2/4 \int_0^{\pi/2} J_2(\alpha \sin \tau) [\exp(i\beta \cos^2 \tau) - 1] \times \cos \tau \sin^3 \tau d\tau, \text{ and}$$

$$G \equiv \alpha^2/4 \int_0^{\pi/2} J_0(\alpha \sin \tau) [\exp(i\beta \cos^2 \tau) - 1] \cos \tau \sin^3 \tau d\tau,$$

where $\alpha = 2kc \sin(\zeta/2)$ and $\beta = (\pi/4)kc(V_0 + iW_0)/E$.

The elastic scattering cross section can then be obtained by multiplying $f(\zeta, \theta, \phi)$ by its complex conjugate and integrating over θ and ϕ ,

$$\begin{aligned} \sigma(\zeta) &= k^2 c^4 \{ |A|^2 + \epsilon [(4/3)|A|^2 + (2/3)\text{Re}(-AB^* + AC^*)] \\ &\quad + (\epsilon^2/5)[2\text{Re}(A[-D^* + (2/3)C^* - (3/2)B^* \\ &\quad - (E^*/3) + F^* - G^*]) + (8/3)|A|^2 + |B|^2 + |C|^2 \\ &\quad + (2/3)\text{Re}(2AC^* - 4AB^* - BC^*)] \}, \quad (6) \end{aligned}$$

where Re means the real part.

The above seven integral expressions were evaluated in series form by expanding the exponentials and identi-

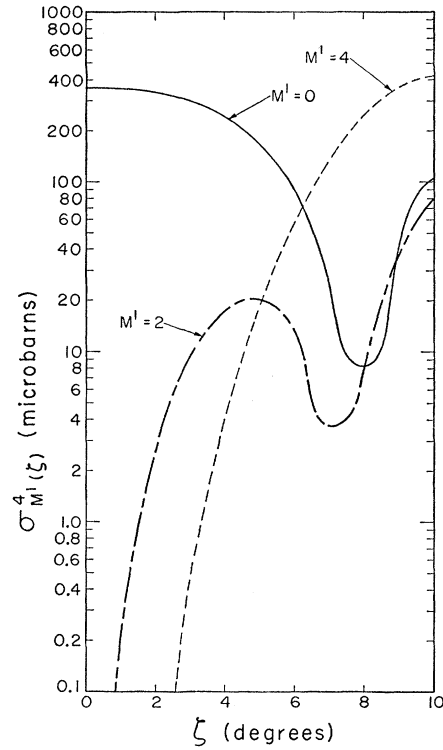
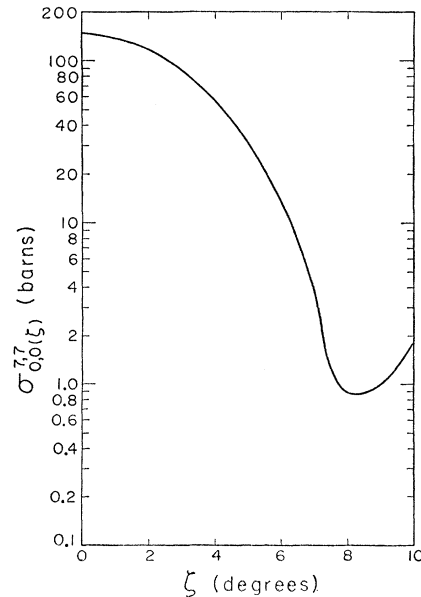


FIG. 11. Rotational scattering of 200-Mev neutrons by lutetium.

fying each of the resulting integrals as one of Sonine's form, whose solution is well known.

Figures 7 and 8 show comparisons of the continuously averaged elastic cross sections with those of the corresponding spherical nuclei. Generally good agreement

FIG. 12. Rotational scattering of 200-Mev neutrons by lutetium, $I=7, M=0$.

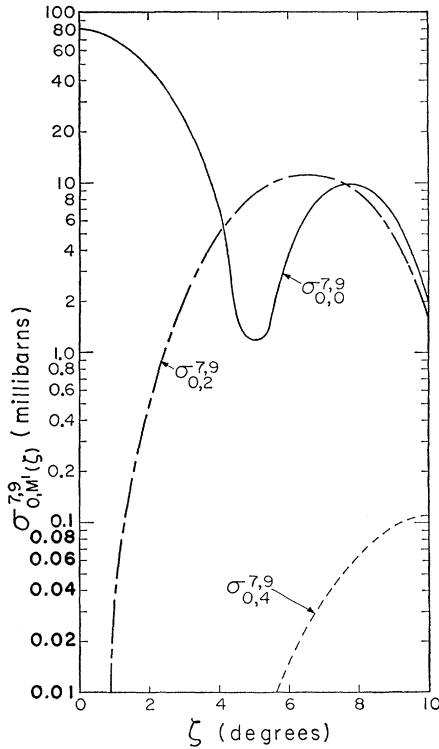


FIG. 13. Rotational scattering of 200-Mev neutrons by lutetium, $I=7$, $M=0$.

appears between the discretely averaged and the continuously averaged cross sections. The only significant effect of the deformation appears to be in the neighborhood of the minima.

Unfortunately, however, these results will be very

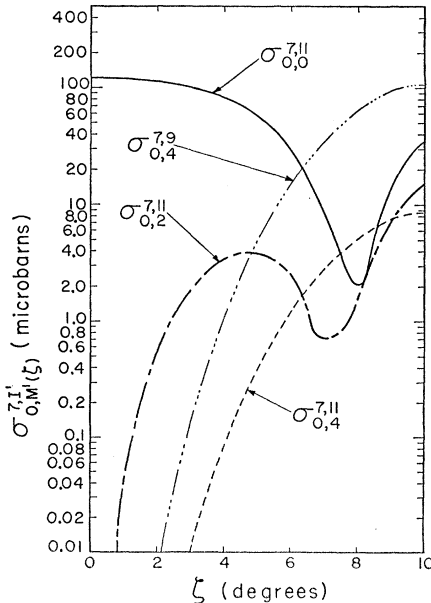


FIG. 14. Rotational scattering of 200-Mev neutrons by lutetium, $I=7$, $M=0$.

difficult to verify experimentally due to the large experimental uncertainties of such differential cross-section measurements. This difficulty is caused partly by the great difficulty in producing a well-resolved beam of high-energy neutrons, and also by the effect of spin-orbit coupling (see Sec. V). Both of these effects tend also to render the minima less pronounced. Such differential cross section measurements for oriented highly deformed nuclei may yield more interesting results, since the calculated curves vary appreciably from one of the three orientations to another, and the position of the minimum also differs.

IV. ROTATIONAL EXCITATION CROSS SECTION

Differential cross sections involving the rotational excitations of the target nucleus will now be investigated entirely quantum mechanically. A technique proposed by Drozdov⁵ will be applied. Inopin⁶ applied this technique to a semitransparent nucleus with a square-well potential.

Drozdov⁵ showed that the differential cross section for rotational excitation from state n_0 to state n is $\sigma_{n_0 n}(\Omega) = |\int \phi_n^*(\omega) f(\omega, \Omega) \phi_{n_0}(\omega) d\omega|^2$, where $f(\omega, \Omega)$ is the scattering amplitude for the nucleus oriented at angle ω with the neutron scattered at angle Ω . $\phi_n(\omega)$ is a rotational eigenfunction. He also defined a summed cross section over all rotational levels: $\sigma_s(\Omega) = \sum_n \sigma_{n_0 n}(\Omega)$. The closure property of $\phi_n(\omega)$ may be applied to obtain $\sigma_s(\Omega) = \int |f(\omega, \Omega) \phi_{n_0}(\omega)|^2 d\omega$. Thus it becomes immediately clear that the latter expression for an initial zero-spin state (constant normalized wave function) is equal to the "elastic" cross section used in Sec. III. However,

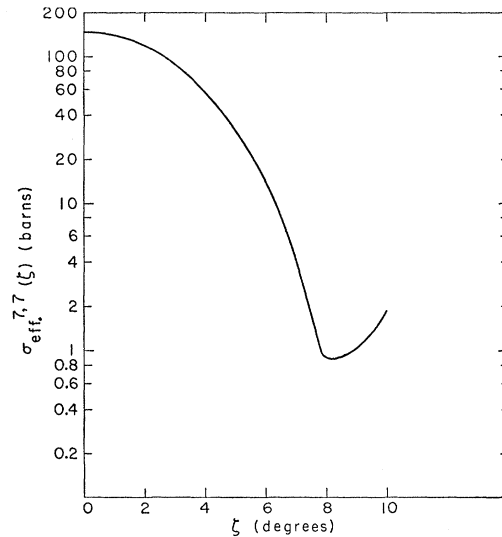


FIG. 15. Rotational cross section for 200-Mev neutrons on lutetium, $\sigma_{\text{eff}}^{7,7}(z) = (1/15) \sum_{M,M'} \sigma_{M,M'}^{7,7}(z)$.

⁵ S. I. Drozdov, J. Exptl. Theoret. Phys. (USSR) **28**, 734 (1955); Soviet Phys. **1**, 591 (1955).

⁶ E. V. Inopin, J. Exptl. Theoret. Phys. (USSR) **30**, 210 (1956); Soviet Phys. **3**, 134 (1956).

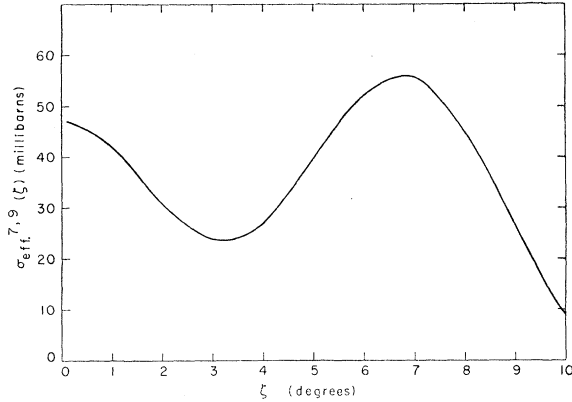


FIG. 16. Rotational cross section for 200-Mev neutrons on lutetium, $\sigma_{\text{eff}}^{7,9}(\xi) = (1/15) \sum_{M, M'} \sigma_{M, M'}^{7,9}(\xi)$.

it can be shown that the elastic cross section is actually the summed cross section for an arbitrary initial-spin state, i.e., state with arbitrary I , M , and K , where I is the nuclear spin, and M and K are its components along space-fixed and nuclear-symmetry axes. The summed

cross section for initial state I, M can be written as an average over initial K states:

$$\begin{aligned} \sigma_{sM}^I(\Omega) &= [1/(2I+1)] \sum_K \sigma_{sM, K}^I(\Omega) \\ &= (1/4\pi) \int_0^{2\pi} \int_0^\pi |f(\Omega, \theta, \phi)|^2 \sin\theta d\theta d\phi. \end{aligned}$$

The rotational wave functions $\phi_n(\omega)$ can be written explicitly as symmetric top eigenfunctions $D_{MK}^I(\phi, \theta, \gamma)$, where γ is the orientation angle of the nucleus about its own symmetry axis.⁷ $\sigma_{n0n}(\Omega)$ can now be written:

$$\begin{aligned} \sigma_{M, K}^I; M', K'(\Omega) &= [(2I+1)(2I'+1)/64\pi^4] \\ &\times \left| \int D_{M'K'}^{I'}(\omega) f(\omega, \Omega) D_{MK}^I(\omega) d\omega \right|^2, \end{aligned}$$

where the unprimed state is the initial state and the primed is the final. Integrating over γ reveals that $K=K'$ for nonvanishing cross sections. Averaging over initial K states and summing over final K states give:

$$\begin{aligned} \sigma_{M, M'}^{I, I'}(\xi) &= [(2I'+1)/4\pi] \sum_{j=|I-I'|}^{I+I'} (I', I, j, M-M' | I', -M', I, M) (I', -M', I, M | I', I, j, M-M') \\ &\times [1/(2j+1)] \left| \int_0^{2\pi} \int_0^\pi Y_{j, M-M'}(\theta, \phi) f(\theta, \phi; \xi) \sin\theta d\theta d\phi \right|^2, \quad (7) \end{aligned}$$

where $(I', I, j, M-M' | I', -M', I, M)$ is a Clebsch-Gordan coefficient.⁷ Initially, for computational simplification an initial spin-zero state was assumed. The rotational cross section then becomes

$$\begin{aligned} \sigma_{0, M'}^{0, I'}(\xi) &= (1/4\pi) \left| \int_0^{2\pi} \int_0^\pi Y_{I', M'}(\theta, \phi) f(\theta, \phi; \xi) \sin\theta d\theta d\phi \right|^2. \quad (8) \end{aligned}$$

The differential cross sections shown in Figs. 9–11 were calculated by using Eq. (8) for a nucleus having dimensions of lutetium. Figures 12–14 were later obtained by using the more general equation (7) for lutetium with $I=7$, $M=0$. It is of interest to note that $\sigma_{0,0}^{7,7}(\xi)$ coincides exactly with $\sigma_{0,0}^{0,0}(\xi)$. Thus the elastic scattering does not depend upon the total spin assigned to the nucleus. The cross-section curves for $I=7$ have the same general qualitative appearance as those corresponding to the case of $I=0$; however, the magnitudes are reduced considerably in all cases except for the elastic scattering.

Finally, M and M' states were respectively averaged and summed over to calculate an effective rotational excitation cross section $\sigma_{\text{eff}}^{I, I'}(\xi)$ for spin states I to I' , as shown in Figs. 15–17.

$$\sigma_{\text{eff}}^{I, I'}(\xi) = \frac{1}{2I+1} \sum_{M, M'} \sigma_{M, M'}^{I, I'}(\xi).$$

Calculations revealed that when the total spin is conserved ($I=I'$) the differential elastic cross section

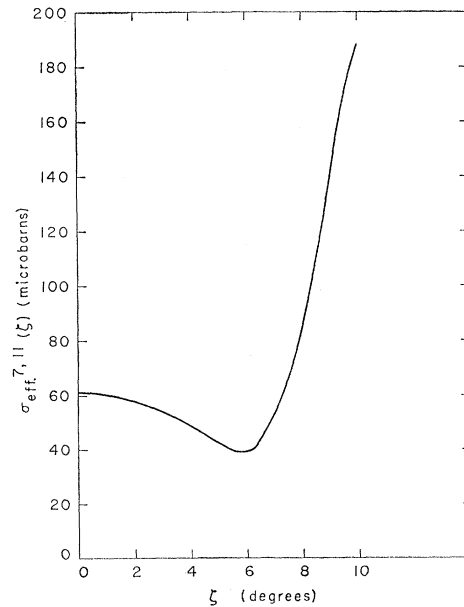


FIG. 17. Rotational cross section for 200-Mev neutrons on lutetium, $\sigma_{\text{eff}}^{7,11}(\xi) = (1/15) \sum_{M, M'} \sigma_{M, M'}^{7,11}(\xi)$.

⁷ A. R. Edmonds, *Angular Momentum in Quantum Mechanics* (Princeton University Press, Princeton, New Jersey, 1957).

$\sigma_{M,M'}^{I,I}(\zeta)$ is the same for all M . This result is expected from purely physical grounds, since the axis along which the azimuthal spin component is quantized can be chosen arbitrarily. Further, $\sigma_{M,M'}^{I,I}(\zeta)$ for cases where $|M-M'|=2$ is smaller than $\sigma_{M,M'}^{I,I}(\zeta)$ by a factor of about 10^3 , and $\sigma_{M,M'}^{I,I}(\zeta)$ for $|M-M'|=4$ is smaller by a factor of about 10^6 . Thus, for $I=I'$ and a given M , the effect of summation over $M' \neq M$ states is almost negligible. Thus $\sigma_{\text{eff}}^{I,I}(\zeta)$ very nearly equals $\sigma_{M,M}^{I,I}(\zeta)$ for all M .

V. INCLUSION OF SPIN-ORBIT COUPLING AND NEUTRON POLARIZATION

If spin-dependent forces are present in neutron scattering processes, a partially polarized beam of neutrons results from the scattering. In order that theoretical deductions may include polarization effects, the central potential must be modified by a term which depends upon the spin-orbit interaction. The spin-orbit potential can be regarded as a term additive to the central potential, i.e., $V_n(\mathbf{r}) + V_{\text{so}}(\mathbf{r})\boldsymbol{\sigma} \cdot \mathbf{L}/\hbar$, where $\boldsymbol{\sigma}$ and \mathbf{L} are the neutron spin and angular momentum operators, and $V_{\text{so}}(\mathbf{r})$ is generally used in the Thomas form, which is proportional to the derivative of the central po-

tential. By obtaining a WKB approximation for the modified wave function, it has been found⁸ that the effect of the spin-orbit interaction on Schiff's small-angle scattering integral is that of a term $V_{\text{so}}(\mathbf{r})\boldsymbol{\sigma} \cdot \boldsymbol{\varrho} \times [(\mathbf{k}_0 + \mathbf{k}_f)/2]$ added to the central potential, where $\boldsymbol{\varrho}$ is a radial vector perpendicular to $\mathbf{k}_0 + \mathbf{k}_f$ and of magnitude $(x^2 + y^2)^{1/2}$. The scattering amplitude becomes

$$f = \frac{k}{2\pi i} \int_{-\infty}^{+\infty} \int_{-\infty}^{+\infty} \exp[i(q_x x + q_y y)] \times \left\{ \exp \left[\frac{-ik}{2E} \int_{-\infty}^{+\infty} \left(V_n(x, y, z) + \boldsymbol{\sigma} \cdot \boldsymbol{\varrho} \times \frac{\mathbf{k}_0 + \mathbf{k}_f}{2} V_{\text{so}}(x, y, z) \right) dz \right] - 1 \right\} dx dy.$$

Letting

$$\chi_n(x, y) = \frac{-k}{2E} \int_{-\infty}^{+\infty} V_n(x, y, z) dz,$$

$$\chi_{\text{so}}(x, y) = \frac{-k}{2E} \int_{-\infty}^{+\infty} V_{\text{so}}(x, y, z) dz,$$

it can be shown that

$$f(\mathbf{k}_0, \mathbf{k}_f) = f_n(\mathbf{k}_0, \mathbf{k}_f) + \boldsymbol{\sigma} \cdot \left[\frac{\mathbf{k}_0 + \mathbf{k}_f}{|\mathbf{k}_0 + \mathbf{k}_f|} \times \mathbf{f}_{\text{so}}(\mathbf{k}_0, \mathbf{k}_f) \right],$$

where

$$f_n = \frac{k}{2\pi i} \int_{-\infty}^{+\infty} \int_{-\infty}^{+\infty} e^{i(q_x x + q_y y)} \left[e^{i\chi_n(x, y)} \cos \left((x^2 + y^2)^{1/2} \left| \frac{\mathbf{k}_0 + \mathbf{k}_f}{2} \right| \chi_{\text{so}}(x, y) \right) - 1 \right] dx dy,$$

and

$$\mathbf{f}_{\text{so}} = -\frac{k}{2\pi} \int_{-\infty}^{+\infty} \int_{-\infty}^{+\infty} e^{i(q_x x + q_y y)} \left[\frac{\boldsymbol{\varrho}}{\rho} e^{i\chi_n(x, y)} \sin \left((x^2 + y^2)^{1/2} \left| \frac{\mathbf{k}_0 + \mathbf{k}_f}{2} \right| \chi_{\text{so}}(x, y) \right) \right] dx dy.$$

Recognizing that $f(\mathbf{k}_0, \mathbf{k}_f)$ is now a 2×2 matrix, the differential cross section becomes $\frac{1}{2} \text{Tr}(f^\dagger f)$, where Tr indicates the trace of the matrix and the dagger (\dagger) indicates the Hermitian conjugate. For an initially unpolarized beam, $\sigma(\zeta, \theta, \phi) = |f_n|^2 + |\mathbf{f}_{\text{so}}|^2$. For spherically symmetric scattering potentials, \mathbf{f}_{so} lies in the scattering

plane. However, for nonvanishing deformations and arbitrary orientations, \mathbf{f}_{so} will generally have a component perpendicular to the scattering plane.

For an initially unpolarized beam, the polarization component in the direction of an arbitrary unit vector \mathbf{n} can be defined⁸ as

$$P(\zeta, \theta, \phi) = \left\{ \frac{1}{2} \text{Tr} \left[f^\dagger \left(\frac{1 + \boldsymbol{\sigma} \cdot \mathbf{n}}{2} \right) f \right] - \frac{1}{2} \text{Tr} \left[f^\dagger \left(\frac{1 - \boldsymbol{\sigma} \cdot \mathbf{n}}{2} \right) f \right] \right\} / \frac{1}{2} \text{Tr}(f^\dagger f),$$

where $(1 \pm \boldsymbol{\sigma} \cdot \mathbf{n})/2$ are projection operators for selecting the spin in the directions $\pm \mathbf{n}$. $P(\zeta, \theta, \phi)$ can be simplified to equal

$$\text{Tr}(f^\dagger \boldsymbol{\sigma} f) \cdot \mathbf{n} / \text{Tr}(f^\dagger f),$$

which becomes

$$2 \frac{\mathbf{k}_0 + \mathbf{k}_f}{|\mathbf{k}_0 + \mathbf{k}_f|} \times \text{Re}(f_n \mathbf{f}_{\text{so}}^*) \cdot \mathbf{n} / (|f_n|^2 + |\mathbf{f}_{\text{so}}|^2).$$

For a spherically symmetric scatterer, the polarization will be directed perpendicular to the scattering plane. However, for nonvanishing deformations and

arbitrary orientations, a component of \mathbf{f}_{so} perpendicular to the scattering plane may yield a polarization component that lies in the scattering plane. However, upon averaging over orientations, such a component vanishes.

ACKNOWLEDGMENTS

This work was performed at the Graduate School of the University of Kansas. I wish to express my appreciation to Dr. William R. Wright of the University of Kansas for his many helpful suggestions and criticisms during the course of this work.